Published in final edited form as:
AJR Am J Roentgenol. 2008 June ; 190(6): 1534–1540. doi:10.2214/AJR.07.3123.

Magnetic Resonance Elastography of Liver Tumors- Preliminary Results

Sudhakar K Venkatesh[1,3], **Meng Yin**[1], **James F Glockner**[1], **Naoki Takahashi**[1], **Philip A Araoz**[1], **Jayant A Talwalkar**[2], and **Richard L Ehman**[1]

[1]Department of Radiology, Mayo Clinic and Foundation, Rochester, MN 55905, USA.

[2]Department of Gastroenterology and Hepatology, Mayo Clinic and Foundation, Rochester, MN 55905, USA.

[3]Diagnostic Radiology, Yong Loo Lin School of Medicine, National University of Singapore, 119074, Singapore.

Abstract

Aim—To evaluate the potential value of magnetic resonance elastography (MRE) for characterizing solid liver tumors.

Materials and Methods—Forty-four liver tumors (metastases-14, hepatocellular carcinoma- 12, hemangioma-9, cholangiocarcinoma-5, focal nodular hyperplasia-3, and hepatic adenoma-1) were evaluated with MRE. MRE was performed on a 1.5 T scanner with a modified phase-contrast, gradient echo sequence to collect axial wave images sensitized along the through-plane motion direction. The tumors were identified in T2-, T1-weighted and gadolinium enhanced T1-weighted images and the MRE images were obtained through the tumor. A stiffness map (elastogram) was generated by an automated process using an inversion algorithm. The mean shear stiffness of the tumor was calculated using a manually specified region of interest placed over the tumor in the stiffness map. The stiffness value of non-tumor bearing hepatic parenchyma was also calculated. Statistical analysis was performed on the stiffness values for differentiation between normal liver, fibrotic liver, benign tumors and malignant tumors.

Results—Malignant liver tumors had significantly higher mean shear stiffness than benign tumors, fibrotic liver and normal liver (10.1kPa vs. 2.7kpa ($p<0.001$), vs. 5.9kPa ($p<0.001$) and vs. 2.3kPa ($p<0.001$) respectively). Fibrotic livers had stiffness values overlapping both the benign and malignant tumors. Cut-off values of 5kPa accurately differentiate malignant tumors from benign tumors and normal liver parenchyma in this preliminary investigation.

Conclusions—MR elastography is a promising, non-invasive technique for assessing solid liver tumors. MRE may provide new, quantitative tissue characterization parameters for differentiating benign and malignant liver tumors.

Introduction

Tumors are frequently detected through physical palpation as hard masses located within softer surrounding tissue [1]. Palpation assesses the tendency of tissue to resist deformation, a physical property of tissue known as elasticity, which varies over a much wider range than other physical properties such as x-ray absorption or MR relaxation times [2,3]. It is generally agreed that no other physical parameter of tissue changes with physiological and pathological

Correspondence, Richard L Ehman, 200, First Street SW, Rochester, MN 55901, USA, Ehman.Richard@mayo.edu, Phone: 1-507-284-7573, Fax: 1-507-284-9778.

process to as great an extent as its elasticity [4]. Researchers have developed imaging techniques using ultrasound [5] and MRI [6] to non-invasively assess the mechanical properties of tissues. This field known as elastography measures internal displacement or strains in tissue that result from application of a static, quasi-static or dynamic stress to that tissue.

Ultrasound based elastography which uses static stress as a probe has been shown to be useful in the differential diagnosis of breast, thyroid and prostate cancers [7–9] and recently in metastatic cervical lymph nodes [10]. However, the technique does not provide a quantitative measurement of tissue elastic modulus.

Magnetic resonance elastography (MRE) is a phase-contrast-based MRI technique that can directly visualize and quantitatively measure propagating mechanical shear waves in biological tissues [6,11,12]. The technique spatially maps and measures the shear wave displacement patterns. The wave images are processed to generate local quantitative values of shear modulus of tissues in maps, known as elastograms [4].

MRE has recently been shown to be useful for non-invasive assessment of liver fibrosis [13, 14] . Studies have demonstrated that MRE can be used to differentiate normal liver from fibrotic liver with a very high degree of accuracy and that the technique is also promising for evaluating the stage of liver fibrosis[15]. In other applications, MRE has been found to have promise for differentiating benign breast lesions from malignant tumors [16,17]. Aside from one publication describing MRE of the brain tumors [18], there have been few reports of the use of MRE to evaluate masses in other parts of the body.

Inspired by the successful application of MRE in non-invasive evaluation of fibrosis of liver at our clinical practice, we sought to evaluate the utility of MRE in characterizing liver tumors.

Non-invasive characterization of focal liver lesions is typically based on the appearance of lesions on pre-contrast T1 and T2 weighted sequences as well as on the dynamic enhancement patterns of lesions following bolus injections of gadolinium-based contrast agents. MRE can be performed following contrast-enhanced MRI so that immediate elastographic analysis of enhancing lesions detected on MRI is feasible. Our main aim of the study was to determine the feasibility of MRE of liver tumors in vivo and their characterization. The main hypothesis of this study was that MRE can depict elastic properties of solid liver tumors and that malignant liver tumors show high shear stiffness compared with normal liver tissue.

Materials and Methods

This study was supported from NIH grant. E01981. This Health Insurance Portability and Accountability Act-complaint study was approved by the IRB of our institute and waived the requirement for informed consent for retrospective data analysis. MRE sequence was performed as a clinical application along with routine conventional MRI study of the liver. Patients gave informed consent as a routine procedure for all MRI studies.

Patients

Between January 2007 and July 2007, 29 patients (16 males and 13 females; mean age 56.8 years, range 18–78 years) with solid liver masses detected with contrast enhanced MRI study were recruited for the MRE study. The indications for MR examination in these patients were: follow-up of a chronic liver disease, evaluation of suspected lesions on sonography or CT, and preoperative staging or follow-up of a known primary malignant tumor elsewhere.

In patients with multiple tumors, we excluded tumors smaller than 10mm to avoid partial volume effects and targeted the largest tumors wherever possible. We excluded tumors smaller

than 10mm to avoid partial volume effects with surrounding liver parenchyma. Eight metastases (in 2 patients) were excluded from the study as the MRE images did not include these metastatic lesions. Two hepatocellular carcinomas (in 2 patients) previously treated with chemoembolization were excluded from the study. The final study group of 44 liver tumors comprised of 12 hepatocellular carcinomas (HCC), 14 metastases, 9 hemangiomas, 5 cholangiocarcinomas, 3 focal nodular hyperplasia's (FNH), and 1 hepatic adenoma. The liver masses ranged from 1.4 to 11cm in maximal diameter (mean, 3.8cm). Final diagnoses of primary liver tumors were established with biopsy or surgery in 4 HCCs, 5 cholangiocarcinomas, 1 FNH, and 1 hepatic adenoma. The diagnosis in 8 HCCs were was based on the widely accepted imaging criteria (presence of a nodule >2cm in diameter and showing characteristic arterial phase hypervascularity on two imaging modalities CT or MR or when the tumor nodule shows arterial phase hypervascularity and venous phase washout, only a single imaging modality is required for the diagnosis) recommended by the European Association for the Study of liver (EASL) conference and the American Association for the Study of Liver Diseases (AASLD) [19,20]. The diagnosis was made by experienced attending radiologists and gastroenterologists. Hemangiomas were diagnosed based on their typical appearances on pre-and post-contrast T1- and T2-weighted MR imaging and using supportive CT or ultrasound imaging, and lesion stability on serial imaging and clinical observation (mean period, 22.6 months, range, 6–38 months). The diagnosis of metastases was based on the surgical and histopathological findings in all 5 patients. The primaries were colonic cancer in 2 patients and intestinal neuroendocrine carcinoma in 2 patients. The primary site was unknown in one patient with type I neurofibromatosis and multiple neuroendocrine carcinoma metastases. Overall the histological proof was available in 7 metastatic nodules (neuroendocrine carcinoma-5 and colonic carcinoma-2). Two colonic carcinoma metastases were confirmed with uptake on FDG-PET scan, surgical palpation and intra-operative ultrasound. The remaining five neuroendocrine carcinoma metastases were confirmed with avid Somatostatin uptake on the Octreotide scans. Sixteen patients had history of diffuse liver parenchymal disease or liver cirrhosis. The causes of liver fibrosis were hepatitis C (n=3), hepatitis B (n=3), primary sclerosing cholangitis (n=1), non-alcoholic steatohepatitis (n=2), cryptogenic (n=4), alcohol abuse (n=2), and primary biliary cirrhosis (n=1). Histologic confirmation of fibrosis/cirrhosis was available in 7 patients (METAVIR score; grade1-1, grade 2-1, grade 3-2, grade 4-3). In the remaining patients with diffuse liver disease, the diagnosis of liver fibrosis was made based on presence of a risk factor, demonstration of nodularity and/or cirrhotic changes on imaging (9 patients), signs of portal hypertension: splenomegaly (7 patients), portosystemic collaterals (2 patients), raised serum liver enzymes (8 patients) and raised aspartate aminotransferase-to-platelet ratio index (APRI) >1 (6 patients) and presence of esophageal varices on endoscopy in one patient. Thirteen patients did not have any history of chronic liver disease, no known risk factors and liver parenchyma did not show any nodularity or cirrhotic configuration on MR Imaging. Also these patients had normal serum liver enzymes and APRI <1. The liver parenchyma in these patients was regarded as normal. Diffuse mild to moderate fatty change was noted in 12 patients and geographical fatty change in one patient. No peritumoral fatty change was demonstrated in our study group. Correlation of fatty change with stiffness values were not done in this study as previous studies have demonstrated that it does not affect stiffness measurement [15].

Imaging technique

MRI was performed on 1.5 T MR Scanners (Signa, General Electric Medical Systems, Milwaukee, WI) with a phased-array torso coil. The standard liver imaging protocol included the following sequences: coronal single shot fast spin echo T2 weighted sequence, respiratory triggered fast spin echo T2-Weighted sequence and/or axial breath hold fast recovery fast spin-echo T2 weighted sequence, axial dual echo in- and out-of phase spoiled gradient echo sequence, axial dynamic 3D fat saturated spoiled gradient echo sequence (LAVA, liver

acquisition with volume acceleration) before and after administration of constrast agent and delayed 2D axial fast spoiled gradient echo sequence. Gadodiamide (Omniscan, Amersham Health) 0.1mmol/kg or Gadobenate dimeglumine (Multihance, Bracco) 0.05mmol/kg was injected intravenously at a rate of 2–3ml/s using an automated injector (MedRad, Pittsburg, PA) and was followed by a 30mL saline flush. Arterial, portal venous and delayed phase images were obtained in all patients. A 2ml test bolus was performed to determine the scan delay following contrast injection to optimize the arterial phase acquisition. All the sequences were performed with patient holding breath in end-inspiration.

MR Elastography

MRE was performed at the end after the standard MRI protocol. An in-house developed 19-cm diameter and 1.5cm thick cylindrical passive driver was placed against the right chest wall overlying the liver and its center at the level of xiphisternum. The passive driver was held in place with an abdominal binder. A continuous acoustic vibration at 60Hz, which was transmitted from an active driver to the passive driver via a flexible vinyl tube, was used to produce propagating shear waves in the liver. A test vibration was first applied on the patient in order to familiarize the patient with the vibration [11]. The MRE sequence was performed either with body or torso array coil. The choice of the coil was determined by the patient size and to accommodate the passive driver. The passive driver can be easily introduced between the patients' chest /abdominal wall and the phased array coil without any effect on image quality. However, in some large sized patients, where it was not possible to do MRI or MRE with a phased array coil, we performed MRE with body coil alone. The propagating shear waves were imaged with a modified phase-contrast, gradient echo sequence (MRE sequence) to collect axial "wave" images sensitized along the through-plane motion direction. The sequence parameters were: TR/TE= 100/25.6ms; bandwidth= ±31.25 kHz; flip angle= 30, FOV= 32–42cm; matrix 256× 96; slice thickness 6–10mm; gap 2mm. There was no special limitation on the field of view for MRE sequence. Four to eight MRE slices were obtained in each patient. The total acquisition time was split into 4 periods of suspended respiration of 16seconds to obtain wave images at 4-phase offsets. In order to obtain a consistent position of the liver for each phase offset, patients were asked to hold their breath at the end of expiration. The tumors were identified by T2- and contrast-enhanced T1-weighted MR images and the MRE slice was targeted to the tumor. The slices which demonstrated the largest cross-section of the tumor were selected. All tumors within the slice were analyzed. The slice thicknesses were 6–10mm, modified according to the size of the focal lesion studied. The smallest tumor was 14mm and the larges 110mm. We excluded tumors smaller than 10mm for there may be partial volume effect with the surrounding liver parenchyma.

MR Elastogram generation

MR elastograms of the liver were obtained by processing the acquired images of propagating shear waves with previously described local frequency estimation (LFE) inversion algorithm [4,21]. The LFE algorithm combines local estimates of instantaneous spatial frequency over several scales to provide robust estimates of shear stiffness. A Gaussian band pass filter was applied to the original wave data to remove low-frequency wave information due to longitudinal waves and bulk motion, and high frequency noise. The cut-off frequencies of the band pass filter were carefully chosen to be far away from the dominant spatial frequencies observed in the liver data. The high end spatial frequency cut-off value is 0.95 cm-1 that corresponds to stiffness values around 0.4 kPa, while the low-end cut-off value is 0.125 cm-1 that corresponds to stiffness values above 23 kPa. Prior to applying the LFE inversion algorithm, we used 8 motion direction filters [22] evenly spaced between 0° and 360° and combined in a weighted least-square method to improve the performance of the algorithm, since complex interference of shear waves from all directions might produce areas with low shear displacement amplitude. All of these processing steps can be applied automatically,

without human intervention, to yield quantitative images of tissue shear stiffness maps, in units of kilopascals.

Mean shear stiffness of the tumor was calculated using a manually specified region of interest (ROI). The ROI was placed by one reader (SKV) who was not aware of the final diagnosis of the solid tumors. The reader was experienced in reading the MR Elastography images and the elastograms. The ROIs were oval or circular and covered most of the tumor in the magnitude image obtained with the MRE sequence and then copied to the stiffness map which gave the stiffness values in kilopascals. We treated each individual lesion to have its own characteristics and calculated shear stiffness of each individual tumor nodule studied. The stiffness values of non-tumor bearing hepatic parenchyma were also calculated by placing multiple ROIs (at least 3) in the parenchyma away from the tumors (2–3 cm). Every attempt was made to take the values in the image which showed the non tumor bearing liver parenchyma most and preferably the slice which did not show any tumor. The ROIs were circular, 1–3 cm in diameter and were placed in the region of the parenchyma excluding vessels. The mean value from multiple ROI was calculated.

Statistical Analysis

Statistical analysis was performed with commercially available software (SAS version 9.01, SAS Institute, Gary, NC). One-way ANOVA analysis was performed for comparison of four different groups of tissues- normal, fibrotic, benign and malignant. Pair-wise comparison was done for different groups and tumor type using Waller-Duncan method for correcting multiple comparisons. We regarded each individual tumor nodule to have its own characteristics and shear stiffness was shown more related to tumor type rather than the individual. We focused on the tumor and did not take into account the differences from the individuals. The overall level of statistical significance was set at $\alpha = 0.05$.

Results

MRE was technically successful in all the 44 lesions studied. There was good illumination of all the liver tumors in the wave images. The patients tolerated the examination well and no adverse effects were reported.

Malignant liver tumors had significantly higher mean shear stiffness than benign tumors (10.1kPa (95% confidence interval (CI), 8.7 – 11.4) vs. 2.7kPa (95% CI, 2.4 – 3.0) ($p<0.001$). Malignant tumors also had significantly higher shear stiffness than normal liver parenchyma and fibrotic liver parenchyma (2.3kPa (95% CI, 2.1 – 2.4) ($p<0.001$) and 5.9kPa (95% CI, 4.5 – 7.2) ($p<0.001$) respectively) (Table 1). Fibrotic livers were significantly stiffer than benign tumors ($p<0.001$) and normal liver tissue ($p<0.001$). The mean stiffness of benign tumors was not significantly different from that of normal liver parenchyma ($p=0.13$).

Cholangiocarcinomas and HCCs had significantly higher stiffness than fibrotic liver, benign tumors and normal liver parenchyma. Metastatic tumors were not significantly stiffer than fibrotic liver, but stiffer than all benign tumors and normal liver parenchyma. Cholangiocarcinoma had significantly higher mean stiffness than HCCs and metastases (16.2kPa vs. 10.3kPa, $p<0.001$ and 7.6kPa, $p<0.001$, respectively) (Table 2). HCCs were significantly stiffer than metastases ($p<0.001$).

Among the benign tumors, hepatic adenoma had the highest stiffness but not significantly different from hemangiomas, FNH, normal liver parenchyma and fibrotic liver. Similarly FNH had stiffness values overlapping the other benign tumors and normal liver. Hemangiomas, however had significantly lower shear stiffness (2.7kPa, 95% CI, 2.3 –3.1) as compared to

fibrotic liver ($p<0.001$). The stiffness of hemangiomas was not significantly different from normal liver.

A cut-off value of 5kPa could accurately (100%) differentiate malignant tumors from benign tumors and normal liver parenchyma. The range of stiffness values of fibrotic livers overlapped the malignant tumors over a wide range. There was minimal overlap of the stiffness values of the fibrotic liver and those of benign tumors.

A linear correlation between size of the lesion and shear stiffness values was noted, but this trend is not significant. ($R^2= 0.20$)

Discussion

Our preliminary study results shows that MRE is feasible for imaging and characterizing solid liver tumors. Malignant liver tumors had higher stiffness values than benign tumors and normal liver parenchyma. Our study results suggest that a threshold value of approximately 5.0 kPa may be useful for differentiating benign focal masses from malignant tumors. However, in the absence of a focal mass stiffness values in liver parenchyma may be higher than 5.0kPa due to liver fibrosis or cirrhosis [15].

The shear stiffness values of normal liver parenchyma and cirrhotic livers in our study are similar to those reported earlier in literature [13–15]. These results demonstrate that MRE is a robust technique for estimation of liver stiffness. Cholangiocarcinomas demonstrated the highest stiffness among the tumors. This was not surprising as these tumors are known to be scirrhous and have a fibrous or desmoplastic stroma [23]. Hepatocellular carcinomas were significantly less stiff than cholangiocarcinomas. This difference may be due to fact that some of the HCCs in our study group had fat component and this may have resulted in lower stiffness values in the HCCs. The metastases group in our study had lower stiffness than cholangiocarcinomas and HCCs. The group comprised of colonic and neuroendocrine metastases and these histological types may have lower stiffness values. Although, there appears to be a certain trend for stiffness values among the malignant tumors, studies with larger number of different tumor types are required to establish the stiffness values.

The exact cause of high shear stiffness in the malignant tumors is not known. Tumors proliferate within a mechanically restricted microenvironment, and tissue is a mechanical elastic solid [24]. Tumor rigidity probably reflects an elevation in interstitial tissue pressure and solid stress due to altered vasculature and tumor expansion [25], an increase in the elastic modulus of transformed cells mediated by an altered cytoarchitecture [26] and matrix stiffening linked to fibrosis [24]. Tumor stiffness arises from multiple factors that are complex in nature. Nevertheless, shear stiffness is an important physical property which can identify malignancy.

Benign tumors were significantly less stiff than all the malignant tumors and the fibrotic liver in our study. Non malignant liver masses are increasingly being recognized with the widespread use of imaging modalities such as US, CT and MRI. The majority of these lesions are detected incidentally in asymptomatic patients. Our study results indicate the potential use of MRE for characterization of incidental mass lesions and also for follow up.

We speculate that another potential application may be to assess tumors after treatment to detect response. As MRE is sensitive to show changes in the tumor stiffness, it might be applied to detect changes following specific anti-tumor therapy.

Our study has limitations. First, the sample size is relatively small and benign liver tumors are not well represented. Second, histological proof was not available in each individual tumor nodule. This is a limitation of our study but was unavoidable because it is not a common practice

at our institute to obtain histological proof when imaging criteria for HCC are met. In case of metastases, some of the nodules also did not have histological confirmation but were regarded as metastases as they demonstrated similar features on PET scan and Octreotide scans. Further some of the metastatic nodules were confirmed with surgical palpation and intra-operative ultrasound. All the cases of chronic liver disease did not have histological proof but were diagnosed with laboratory and imaging criteria. We did not attempt to differentiate between different etiologies of liver fibrosis as numbers of cases were small in each etiologic group. However, the results provide motivation for conducting a study with a larger number of lesions with histological proof to confirm the preliminary findings. Third, the MRE technique used in this study has certain technical limitations. Planar wave imaging was performed with 2-dimensional wave inversion. The inversion process therefore does not take into account propagation of waves at an angle relative to the plane of section. Particularly for small structures, this can yield stiffness values that may be incorrectly low due to partial volume effects and edge effects in the inversion algorithm. This occurs whenever the lesion is smaller than the wavelength of the shear wave used. Therefore one may have to use a higher frequency and smaller wavelength acoustic waves to accurately estimate the stiffness of smaller structures. However, high frequency waves get attenuated very fast in the liver posing a limitation for its use. While the results show that even with these limitations the technology shows promise; the best approach in the future may be to employ 3-dimensional acquisition and inversion of wave data to address these limitations. 3D MRE can be performed with four phases or 2 phases. These techniques are currently under development at our lab.

In conclusion, MRE is a feasible technique for quantitatively evaluating the mechanical properties of liver masses, offering new parameters for tissue characterization with MRI. The technique can be readily combined as a complement to conventional MRI of the abdomen. MRE shows promise for improving characterization of liver tumors.

Acknowledgments

This publication was supported by NIH grant EB001981

The authors would like to acknowledge Mr. Stephen S Cha, Biostatistics, Mayo Clinic, Rochester, for his assistance in statistical analysis.

References

1. Paszek MJ, Zahir N, Johnson KR, et al. Tensional homeostasis and the malignant phenotype. Cancer Cell 2005;8:241–254. [PubMed: 16169468]
2. Duck, FA. Physical Properties of Tissue- a Comprehensive Reference Book. San Diego, CA: Academic; 1990. p. 225-248.
3. Sarvazyan AGD, Maevsky E, Oranskaja G, Mironova G, Sholokhov V, Ermilova V. Elasticity imaging as a new modality of medical imaging for cancer detection. Proceedings of an International Workshop on the Interaction of Ultrasound with Biological Media 1994:68–81.
4. Manduca A, Oliphant TE, Dresner MA, et al. Magnetic resonance elastography: non-invasive mapping of tissue elasticity. Med Image Anal 2001;5:237–254. [PubMed: 11731304]
5. Ophir J, Cespedes I, Ponnekanti H, Yazdi Y, Li X. Elastography: a quantitative method for imaging the elasticity of biological tissues. Ultrason Imaging 1991;13:111–134. [PubMed: 1858217]
6. Muthupillai R, Lomas DJ, Rossman PJ, Greenleaf JF, Manduca A, Ehman RL. Magnetic resonance elastography by direct visualization of propagating acoustic strain waves. Science 1995;269:1854–1857. [PubMed: 7569924]
7. Garra BS, Cespedes EI, Ophir J, et al. Elastography of breast lesions: initial clinical results. Radiology 1997;202:79–86. [PubMed: 8988195]
8. Cochlin DL, Ganatra RH, Griffiths DF. Elastography in the detection of prostatic cancer. Clin Radiol 2002;57:1014–1020. [PubMed: 12409113]

9. Lyshchik A, Higashi T, Asato R, et al. Thyroid gland tumor diagnosis at US elastography. Radiology 2005;237:202–211. [PubMed: 16118150]
10. Lyshchik A, Higashi T, Asato R, et al. Cervical lymph node metastases: diagnosis at sonoelastography--initial experience. Radiology 2007;243:258–267. [PubMed: 17293571]
11. Muthupillai R, Ehman RL. Magnetic resonance elastography. Nat Med 1996;2:601–603. [PubMed: 8616724]
12. Ehman RL, Crues JV, Lenkinski RE, et al. Magnetic resonance. Radiology 1996;198:920–926.
13. Rouviere O, Yin M, Dresner MA, et al. MR elastography of the liver: preliminary results. Radiology 2006;240:440–448. [PubMed: 16864671]
14. Huwart L, Peeters F, Sinkus R, et al. Liver fibrosis: non-invasive assessment with MR elastography. NMR Biomed 2006;19:173–179. [PubMed: 16521091]
15. Yin M, Talwalkar JA, Glaser KJ, et al. Assessment of hepatic fibrosis with magnetic resonance elastography. Clin Gastroenterol Hepatol 2007;5:1207–1213. [PubMed: 17916548]
16. McKnight AL, Kugel JL, Rossman PJ, Manduca A, Hartmann LC, Ehman RL. MR elastography of breast cancer: preliminary results. AJR Am J Roentgenol 2002;178:1411–1417. [PubMed: 12034608]
17. Sinkus R, Tanter M, Xydeas T, Catheline S, Bercoff J, Fink M. Viscoelastic shear properties of in vivo breast lesions measured by MR elastography. Magn Reson Imaging 2005;23:159–165. [PubMed: 15833607]
18. Xu L, Lin Y, Han JC, Xi ZN, Shen H, Gao PY. Magnetic resonance elastography of brain tumors: preliminary results. Acta Radiol 2007;48:327–330. [PubMed: 17453505]
19. Bruix J, Sherman M, Llovet JM, et al. Clinical management of hepatocellular carcinoma. Conclusions of the Barcelona-2000 EASL conference. European Association for the Study of the Liver. J Hepatol 2001;35:421–430. [PubMed: 11592607]
20. Bruix J, Sherman M. Management of hepatocellular carcinoma. Hepatology 2005;42:1208–1236. [PubMed: 16250051]
21. Westin CF, Wigstrom L, Loock T, Sjoqvist L, Kikinis R, Knutsson H. Three-dimensional adaptive filtering in magnetic resonance angiography. J Magn Reson Imaging 2001;14:63–71. [PubMed: 11436216]
22. Manduca A, Lake DS, Kruse SA, Ehman RL. Spatio-temporal directional filtering for improved inversion of MR elastography images. Med Image Anal 2003;7:465–473. [PubMed: 14561551]
23. Goodman ZD. Neoplasms of the liver. Mod Pathol 2007;20 Suppl 1:S49–S60. [PubMed: 17486052]
24. Paszek MJ, Weaver VM. The tension mounts: mechanics meets morphogenesis and malignancy. J Mammary Gland Biol Neoplasia 2004;9:325–325. [PubMed: 15838603]
25. Padera TP, Stoll BR, Tooredman JB, Capen D, di Tomaso E, Jain RK. Pathology: cancer cells compress intratumour vessels. Nature 2004;427:695. [PubMed: 14973470]
26. Beil M, Micoulet A, von Wichert G, et al. Sphingosylphosphorylcholine regulates keratin network architecture and visco-elastic properties of human cancer cells. Nat Cell Biol 2003;5:803–811. [PubMed: 12942086]

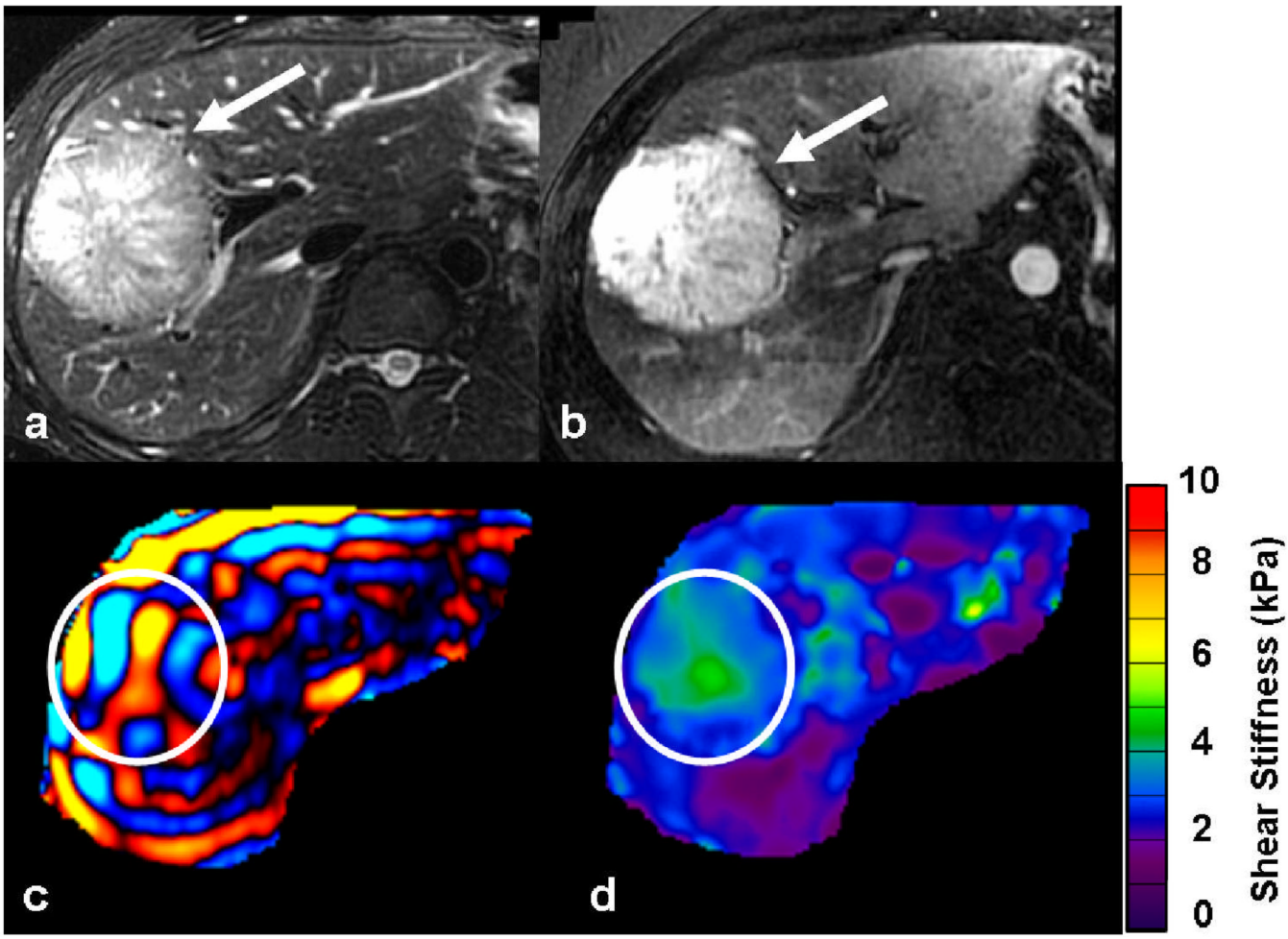

Fig. 1.

39-year-old man with incidental liver tumor. A large tumor in the right lobe of the liver was incidentally detected during an ultrasound examination. The tumor (*white arrow*) is hyperintense on the T2-weighted image (a) and seen to intensely enhance in arterial phase of gadolinium enhanced T1-weighted image (b). Axial MRE wave image (c) showing good illumination of the tumor (ROI). Note that the waves in the tumor have slightly longer wavelength as compared to those in surrounding normal liver parenchyma. Elastogram (d) with ROI corresponding to the tumor. The shear stiffness value of the tumor was 3.1kPa and the surrounding liver, 2.4kPa. Patient underwent right hepatectomy and final diagnosis was hepatic adenoma.

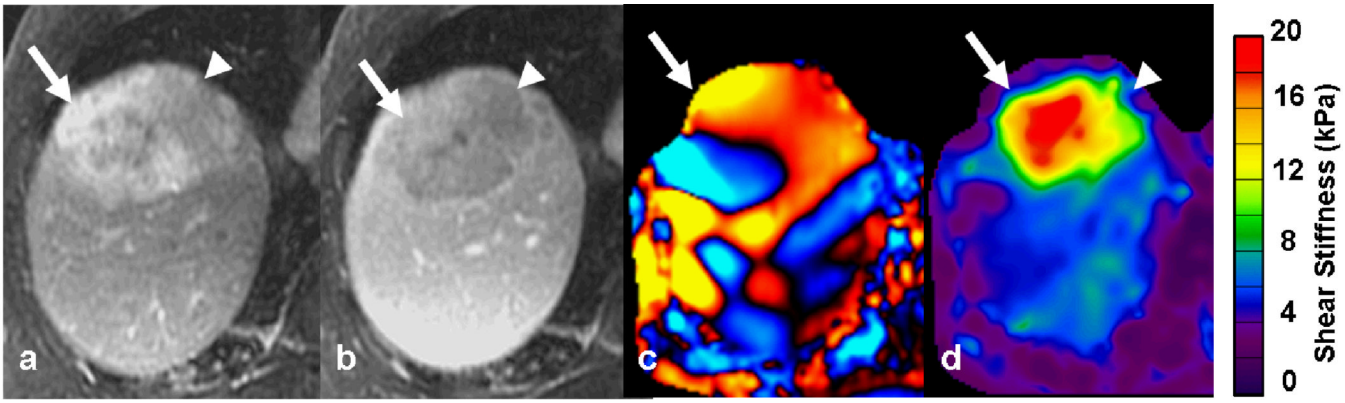

Fig. 2.

78-year-old man with cryptogenic cirrhosis and biopsy proven hepatocellular carcinoma. Post gadolinium-enhanced T1-weighted images showing an enhancing tumor (*white arrow*) in right lobe of the liver during arterial phase (a) with washout in the portal venous phase (b). The MRE wave image (c) shows shear waves with long wavelength within the tumor. The waves in the surrounding liver also have longer wavelength than normal. The mean stiffness of the tumor was 14.2kPa. Note the fat containing region within the tumor (*arrowhead*) which appears less stiff on the elastogram. The liver parenchyma had a stiffness of 4.1kPa consistent with liver fibrosis.

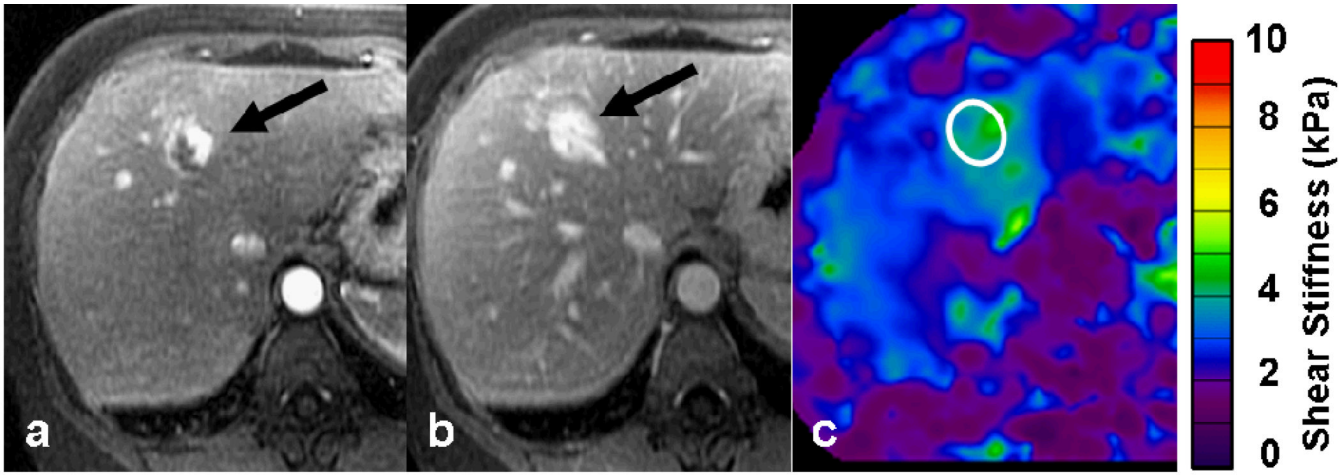

Fig. 3.

51-year-old female with hemangioma in the liver. T1-weighted images in the arterial phase (a) and delayed phase (b) showing a typical hemangioma (black arrow). The stiffness of the hemangioma was 3.2kPa calculated with the ROI placed on the elastogram (c). The normal liver parenchyma had stiffness value of 2.3kPa

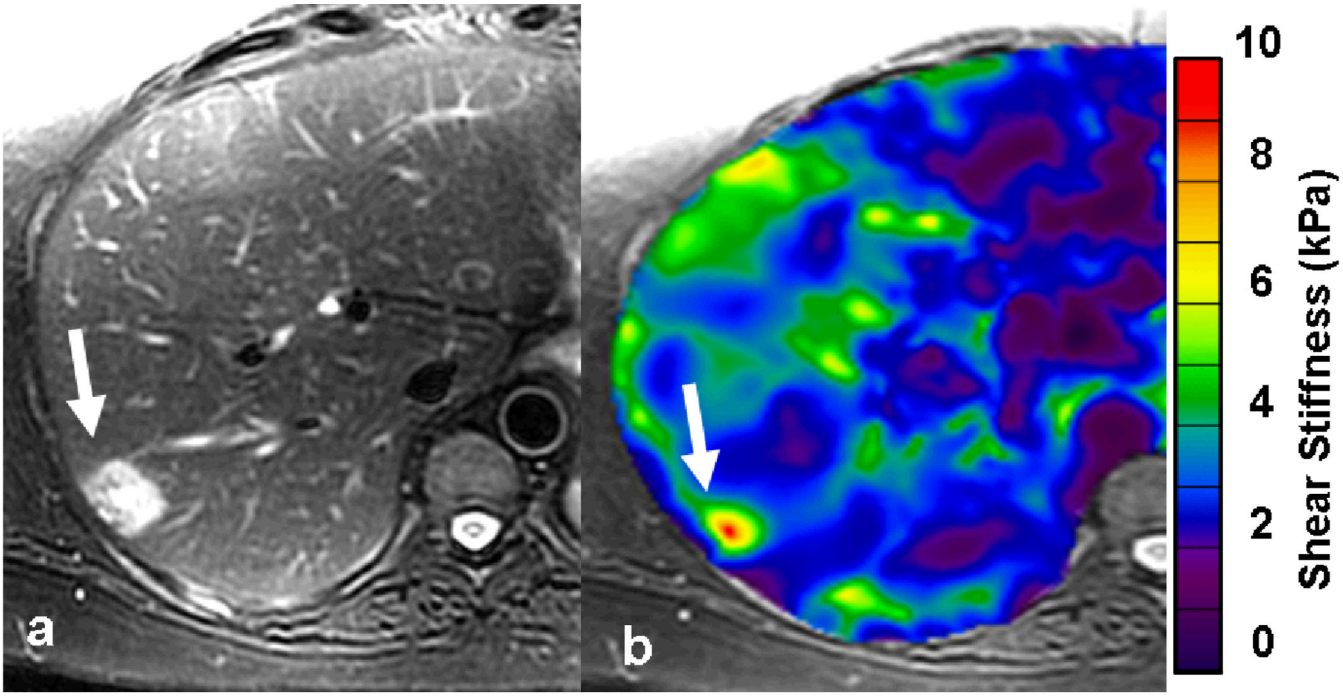

Fig. 4.

55-year-old female with fatty liver and a focal lesion in right lobe. T2-weighted image (a) showing a single hyperintense lesion in the periphery of right lobe of the liver (arrow). Elastogram shows the tumor as a “hot spot” with stiffness value of 6.2kPa suggestive of a malignant tumor. A subsequent colonoscopy revealed a carcinoma in the recto-sigmoid region. Patient underwent surgical resection of the liver tumor and confirmed to be metastases.

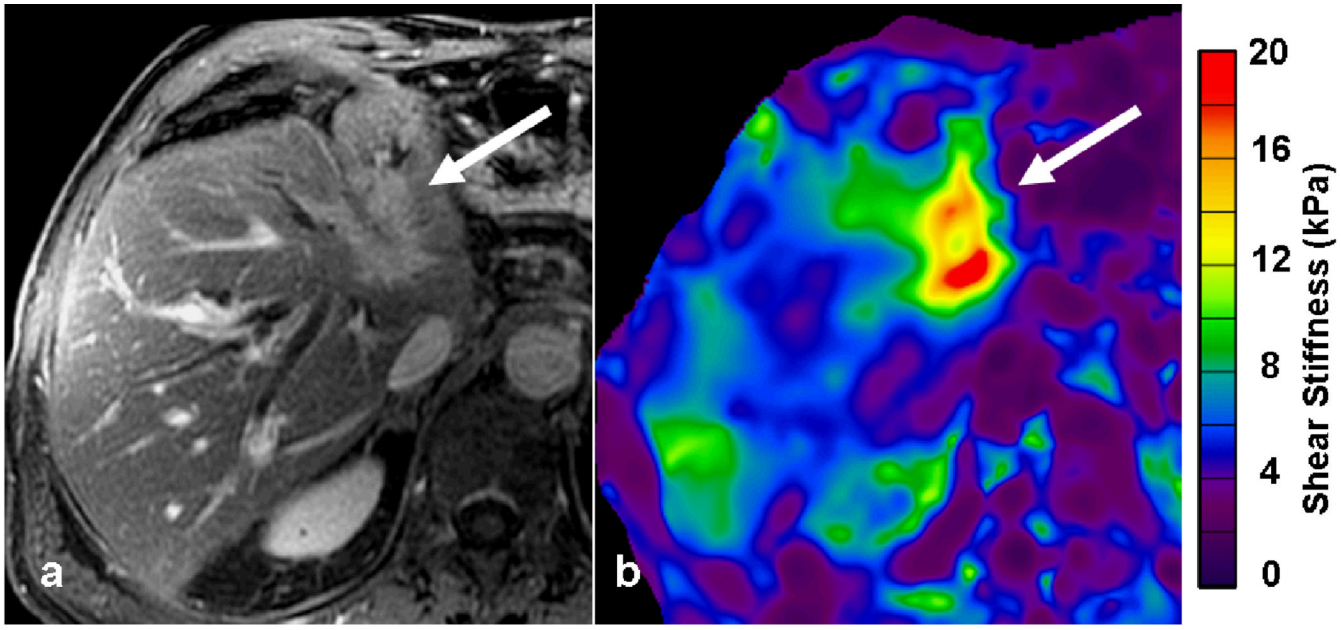

Fig. 5.
77-year-old man with intrahepatic cholangiocarcinoma. Gadolinium enhanced T1-weighted image (a) showing an enhancing tumor involving the left hepatic duct and invading into surrounding left lobe of liver. The mean stiffness of tumor is 15.5kPa and that of liver parenchyma 4.3kPa. Patient underwent biliary stenting and currently on follow-up.

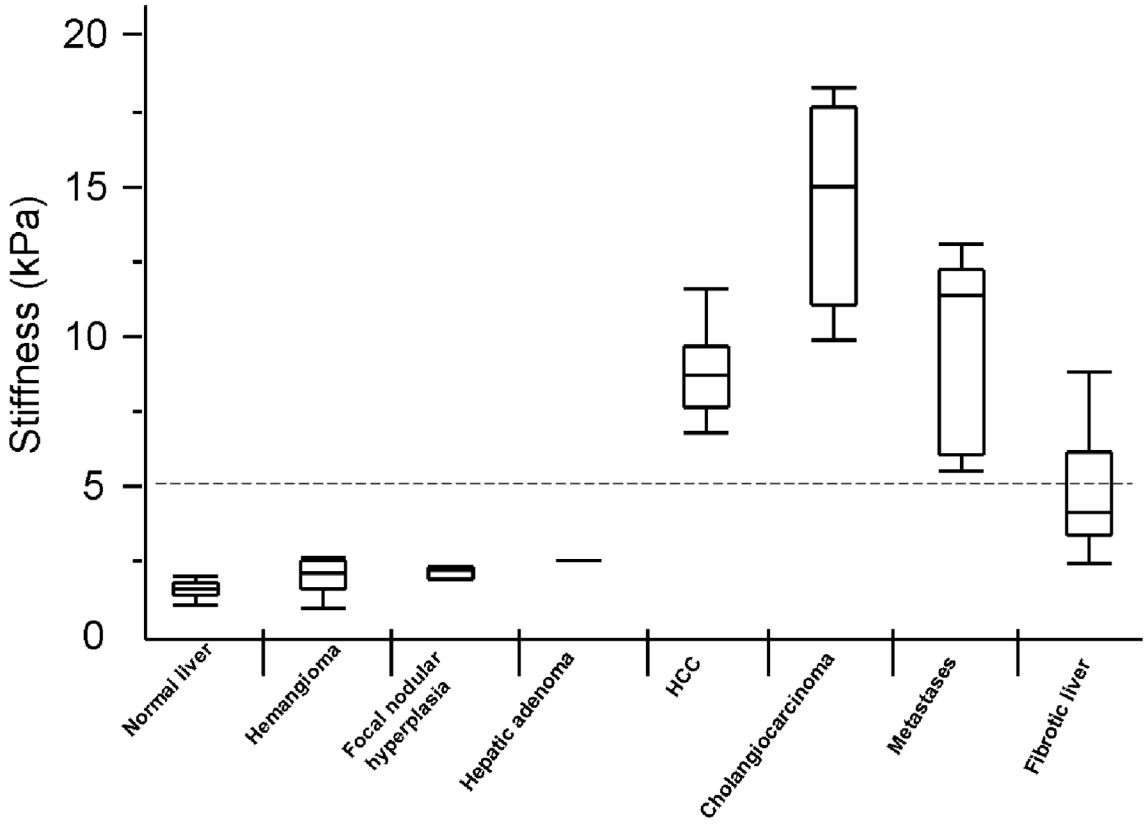

Fig. 6.

Graph showing box plots of shear stiffness of different tissues. A cut-off value of 5kPa separates malignant tumors from benign tumors and normal liver. Note that the stiffness values of fibrotic liver overlaps both benign and malignant tumor.

Table 1

Shear Stiffness Values in Liver Parenchyma and Liver Tumors

Group	*n*	Shear Stiffness (kPa)	
		Mean ± SD	**Range**
Malignant tumors	31	10.1 ± 3.6	6.2 – 19.6
Benign tumors	13	2.7 ± 0.4	1.6 – 3.2
Fibrotic liver	16	5.9 ± 2.5	3.1 – 12.2
Normal liver	13	2.3 ± 0.3	1.8 – 2.8

Table 2

Shear Stiffness Values of Individual Tumor Types

Tumor	*n*	Shear Stiffness (kPa)	
		Mean ± SD	Range
Focal nodular hyperplasia	3	2.7 ± 0.2	2.4 – 2.9
Hemangioma	9	2.7 ± 0.5	1.6 – 3.2
Hepatic adenoma	1	3.1	
Cholangiocarcinoma	5	16.2 ± 3.4	10.8 – 19.6
Hepatocellular carcinoma	12	10.3 ± 2.0	7.6 – 14.2
Metastasis	14	7.6 ± 1.7	6.2 – 12.2